

Adaptive control of dynamic networks

Chunyu Pan¹, Zhao Su², Haoyu Zheng², Changsheng Zhang¹, Weixiong Zhang³ and Xizhe Zhang^{2,4*}

1. Northeastern University, Shenyang 110169, China;

2. School of Biomedical Engineering and Informatics, Nanjing Medical University, Nanjing, Jiangsu 210001, China;

3. Department of Health Technology and Informatics, Department of Computing, The Hong Kong Polytechnic University, Hong Kong, China;

4. Early Intervention Unit, Department of Psychiatry, The Affiliated Brain Hospital of Nanjing Medical University, Nanjing, Jiangsu 210029, China;

*Correspondence: Xizhe Zhang: zhangxizhe@njmu.edu.cn;

Abstract—Real-world network systems are inherently dynamic, with network topologies undergoing continuous changes over time. External control signals can be applied to a designated set of nodes within a network, known as the Minimum Driver Set (MDS), to steer the network from any state to a desired one. However, the efficacy of the incumbent MDS may diminish as the network topologies evolve. Previous research has often overlooked this challenge, assuming foreknowledge of future changes in network topologies. In reality, the evolution of network topologies is typically unpredictable, rendering the control of dynamic networks exceptionally challenging. Here, we introduce adaptive control – a novel approach to dynamically construct a series of MDSs to accommodate variations in network topology without prior knowledge. We present an efficient algorithm for adaptive control that minimizes adjustments to MDSs and overall control costs throughout the control period. Extensive experimental evaluation on synthetic and real dynamic networks demonstrated our algorithm's superior performance over several state-of-the-art methods. Adaptive control is general and broadly applicable to various applications in diverse fields.

Index Terms—Dynamic network; Adaptive control; Driver node; Maximum matching;

I. INTRODUCTION

Complex systems, best represented in networks, are pervasive in many fields, and network analysis is essential for understanding intrinsic system properties [1-3]. For instance, in the biomedical field, analysis of gene regulation and protein interaction in the cell [4-7] provides a paradigm for discovering and interpreting, e.g., molecular pathways and disease mechanisms. In neuroscience, investigating control principles of brain networks [8-10] can help elucidate the underlying mechanisms of brain function and cognition as well as the origins of neurodegenerative diseases and neuropsychiatric disorders. In economics, financial network analysis [11-13] facilitates risk assessment and economic trend prediction.

Network control has attracted much attention lately [14-16]. A network is controllable if external control signals can guide it from an initial state to a desired state [14], with the nodes receiving control signals being referred to as *driver nodes* [17]. The set of the fewest driver nodes is called the Minimum Driver Set (MDS). *Liu* and *Barabási* were among the first to explore the theoretical underpinnings of MDS [14, 17], paving the way for applications and subsequent studies investigating the properties of MDS. *Zhang* et al. proposed an efficient algorithm to discover all possible driver nodes by finding a maximum matching of a given network, moving toward solving many control-related issues in network control [18]. *Ruths* categorized driver nodes into three distinct types to elucidate network control structures to help unveil the essential roles of driver nodes and MDS compositions [19, 20]. Earlier, we presented a novel method for finding preferential matchings to derive MDS with distinct attributes, showing that modifying or removing edges can shift the network's control modes [21-24]. *D'Souza* et al. [15] comprehensively reviewed network control and discussed its inception, the latest development and future research directions. These previous works have set a foundation for selecting optimal MDS.

Despite these achievements, it is important to highlight that the previous studies predominantly considered static networks with fixed topologies, seriously limiting control theory's applicability in practice.

Most real-world networks are inherently dynamic [25, 26], i.e., their topological structures evolve constantly. One approach to controlling a dynamic network is to treat it as a series of static networks and identify the MDS for controlling these static representations. Exploiting this idea, *Posfai* et al. presented a method to investigate the maximum subspace a single driver node

can control in a dynamic network [27]. This method set a cornerstone for many subsequent studies. *Ravandi et al.* expanded this method to a heuristic for finding approximate MDS [28], which is a significant step towards dynamic network control. Moreover, the controllability of dynamic networks has lately become a research focus. *Pan et al.* introduced a graphical approach to unraveling individual controllability mechanisms of large dynamic networks [29]. *Yao et al.* [30] designed several switching strategies to optimize the placement of the controller to improve overall control performance. The results of the controllability of dynamic networks and the selection of MDS set a theoretical basis for our research.

An implicit, albeit fundamental, assumption underlying the existing methods for dynamic networks [27-30] is that any network structural alteration must be known *a priori*, which is typically violated in practice. They treated a dynamic network as a whole and attempted to identify a single MDS capable of controlling the constantly evolving network. These methods assume that an MDS can only be determined after all the dynamic topological changes have been observed. Consequently, control can only be exerted if the network undergoes a predetermined sequence of dynamic changes that will occur in the future – such a scenario may occur only in specific recurrent dynamic networks like artificially designed networks. However, the structures of most real-world networks vary stochastically. Predicting network topological variations is a formidable challenge for most real-world networks. When future network changes are unpredictable, precomputing an MDS suitable for the entire dynamic network is impractical. Therefore, it is imperative to recalculate MDS when the network changes to ensure full network control (Figure 1).

Here, we present a novel control strategy, named *adaptive control*, to address this ground challenge of controlling dynamic networks in real time. The objective of adaptive control is not to control the entire dynamic network *post hoc* but to ensure real-time control of a series of individual snapshots of the dynamic network as they emerge. When a dynamic network undergoes topological changes, the adaptive control strategy reconstructs a new MDS to accommodate these changes, ensuring continued control over the entirety of the dynamic network. This adaptive control approach is markedly different from the previous schemes [27-30]. Our new adaptive control approach hinges upon a novel real-time algorithm for computing and updating MDS. Briefly, we introduce a node control importance metric to optimize MDS. This importance metric incorporates information on historical topological variations and anticipated future network changes, aiming to minimize changes to MDS. We explore this node metric in a partial matching repair algorithm to compute a new MDS that is as consistent as possible with its previous counterpart.

In summary, we make the following contributions:

- (1) We introduce an adaptive control problem, that is, how to reduce the changes in MDS as much as possible without knowing the subsequent changes in the network. In this problem, most of the previous strategies that require prior knowledge of the network topology will fail because they must adjust the current MDS in real time to support emerging network changes and ensure continuous dynamic control with the smallest cost possible.
- (2) We present a new Adaptive Control algorithm (AC) to tackle the fundamental challenges of adaptive control in dynamic networks. The AC algorithm aims to minimize the difference between consecutive MDSs used in the adaptive control of dynamic networks. It selects the most suitable MDS for every consecutive network snapshot, considering its historical topological variations and potential future configurations.

The remainder of the paper is structured as follows: Section 2 defines dynamic networks and describes adaptive control. Section 3 motivates the research and describes the AC algorithm. Section 4 presents empirical results and compares our new method with the existing ones on simulated and real-world networks. Finally, Section 5 concludes and outlines future directions.

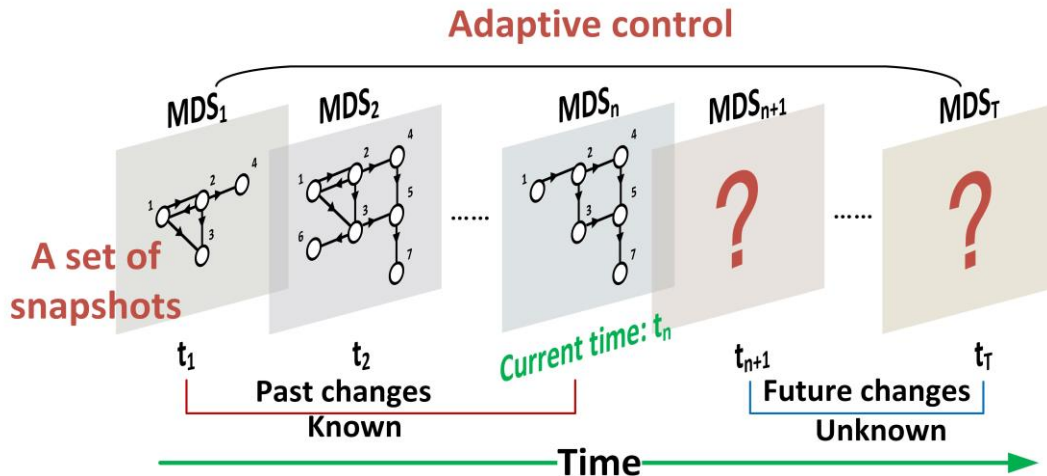


Figure 1. Adaptive control of dynamic networks. At the current time t_n , only the previous network topologies $[t_1, \dots, t_n]$ are available, while the subsequent network topology is unknown. The goal of adaptive control is to compute the current MDS_n in real time to maintain control of the network. As a result, each snapshot will have its own MDS.

II. PROBLEM DEFINITION AND PRELIMINARIES

A. Controllability of dynamic network

A dynamic network can be viewed as a discrete linear time-variant (LTV) system, and following [17, 29], its dynamics can be represented as,

$$\frac{dx(t)}{dt} = A(t)x(t) + B(t)u(t)$$

where vector $x(t) = (x_1(t), \dots, x_N(t))^T \in \mathbb{R}^N$ represents the states of N nodes at time t , $A(t) \in \mathbb{R}^{N \times N}$ denotes the adjacency matrix of the dynamic network at t , $B(t) \in \mathbb{R}^{N \times M}$, $M \leq N$ specifies the nodes to be controlled by the external controller at t , and $u(t) = (u_1(t), \dots, u_M(t))^T \in \mathbb{R}^M$ defines the input on M nodes. The controller uses input $u(t)$ to control the system, and a single control signal can typically drive multiple nodes

We can model the dynamic network G as a series of (unknown) evolving snapshots [31], represented as $G = \{G_1(V_1, E_1), G_2(V_2, E_2), \dots, G_T(V_T, E_T), \dots\}$. Every snapshot is defined over a duration τ . A snapshot during time span $[t, t+\tau)$ is considered as a static *temporal subgraph* $G_t(V_t, E_t)$, where $V_t = \{v_1, v_2, \dots, v_N\}$ and $E_t = \{e_1, e_2, \dots, e_L\}$ represent the sets of nodes and edges that emerge within $[t, t+\tau)$. The system is assumed to spend a finite amount of time in each temporal subgraph [32, 33]. Over extended time horizons, every temporal subgraph is viewed as switching instantaneously to the next subgraph. At the current time t , only the temporal subgraph $G_\varepsilon(V_\varepsilon, E_\varepsilon)$, $\varepsilon \in [1, t]$ is known, where $\varepsilon \in [1, t]$, and topological changes in the upcoming network are unknown (Figure 1)

We are interested in the controllability of temporal subgraphs rather than the entire dynamic network, where a temporal subgraph G_i is described as a static network subject to the canonical linear time-invariant (LTI) dynamics [25]

$$\frac{dx(t)}{dt} = A_i x(t) + B_i u_i(t)$$

According to the Kalman rank condition[34], G_i is controllable if and only if matrix $C = (B, AB, A^2B, \dots, A^{N-1}B)$ is full rank, and the system can be driven from any initial state to any final state in finite time. However, for most real networks, it is untrivial to obtain the weight for every edge. To circumvent this difficulty, *Liu* [14] introduced structural controllability to assess network controllability based on network structures. Structural controllability provides an operational means to determine the minimum number of inputs required to control a network and identify the locations in the network to place the inputs.

In the structural controllability theory, the Minimum Driver node Set (MDS) signifies the smallest node assembly needed to guide a directed network to a desired state. The computation of the MDS is achieved by finding a maximum matching in the bipartite graph of the network [14]. A matching in a network refers to a set of edges sharing no node in common. A maximum matching is a matching with the largest number of edges, which can be found by the Hopcroft-Karp (HK) algorithm [35]. Nodes without directly matched edges pointed to are designated driver nodes [14].

B. Adaptive control of dynamic networks

Consider a dynamic network G , composed of a series of temporal subgraphs $\{G_T(V_T, E_T)\}_{t=1}^T$, where $G_i(V_i, E_i)$ is the i^{th} temporal subgraph at time t . We apply the Hopcroft-Karp [35] algorithm to find a series of MDSs, denoted as $DS = \{D_T\}_{t=1}^T$, for each G_i in G .

The objective of adaptive control is to derive an MDS sequence DS with minimal control costs for the changing network. This implies ensuring that the newly computed MDS is as similar as possible to the previous MDS to exert minimal disruption to the control scheme. To this end, we introduce the Extra Control Cost (*ECC*) to quantify the difference between consecutive MDSs of all consecutive temporal subgraphs:

$$ECC = \sum_{i=1}^T |D_{i+1} - D_i|$$

where, D_t represents the MDS of the t^{th} temporal subgraph, and $|D_t - D_{t-1}|$ is the number of driver nodes belonging to the current MDS but not to the previous one.

In other words, *ECC* quantifies the number of new driver nodes required to adapt to the network changes. Our objective is to minimize *ECC* to reduce overall control costs:

Objective:

$$\text{Minimize } ECC(DS)$$

Subject to:

$$s. t. \begin{cases} DS = \{D_1, D_2, \dots, D_i, \dots\} \\ \forall i, D_i \in \text{All possible MDS of } G_i(V_i, E_i) \end{cases}$$

III. THE METHOD

A. Motivation and two guiding principles

Adaptive control of a dynamic network requires repeatedly recomputing MDSs so that the overall change across consecutive MDSs is minimized as network structures are involved. Note that a temporal subgraph usually contains multiple MDSs [36, 37], each having different driver nodes (Figure 2). Therefore, we can select similar MDSs across adjacent temporal subgraphs to minimize ECC . For instance, Figure 3A shows a dynamic network and its sequential temporal subgraphs. In Figure 3B, the initial MDS of subgraph G_1 includes nodes v_1 and v_2 . As the network evolves to G_2 , the MDS shifts to nodes v_3 and v_4 , indicating a complete change in driver nodes. Over time, the network requires control over eight driver nodes, with a total of nine changes in the MDS. In contrast, Figure 3C represents a more stable MDS sequence with only four driver nodes and merely two changes of driver nodes between consecutive subgraphs. The presence of multiple selectable MDSs within a subgraph opens an avenue to optimizing the overall MDS of a dynamic network.

An effective approach to selecting an MDS for the current temporal subgraph must consider historical network topologies and possible future network changes. Historical topologies can be explored and exploited to estimate future network structures and help reduce ECC in two aspects. First, historically stable nodes, which often appeared in the node sets of the previous temporal subgraphs, are preferred to be included in the current MDS; doing so can minimize swapping in and out driver nodes and stabilize the overall adaptive control of the network. We refer to this consideration as *the stability principle of adaptive control*. Second, when computing the current MDS, we can explore the previous MDS to achieve the maximal consistency between the current and the previous MDSs, thereby minimizing the change to the MDS. We refer to this consideration as *the consistency principle of adaptive control*.

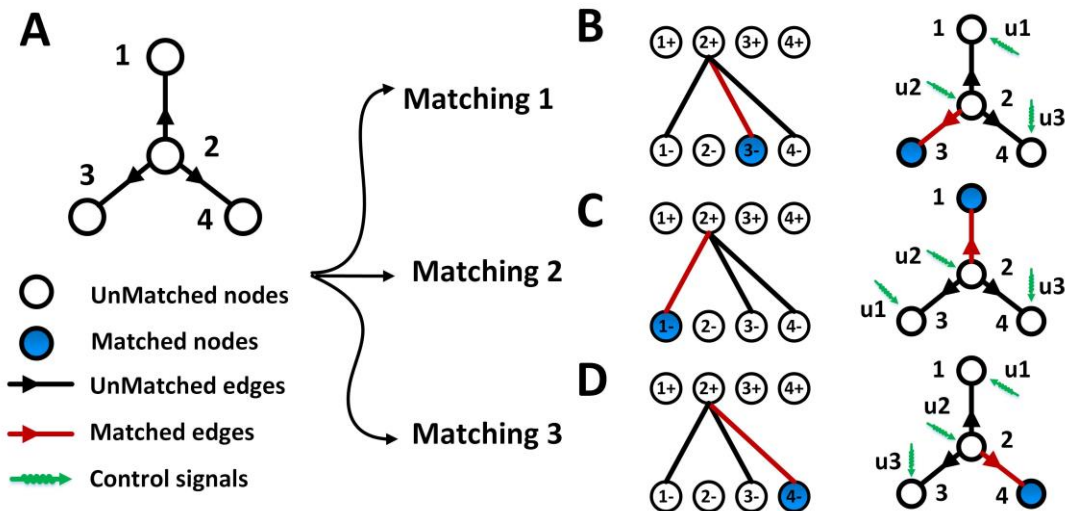


Figure 2. A simple network with three different MDS. (A) A simple network with four nodes and three edges. (B)-(D) Different maximum matchings of the network (A). Different maximum matchings may produce different MDSs.

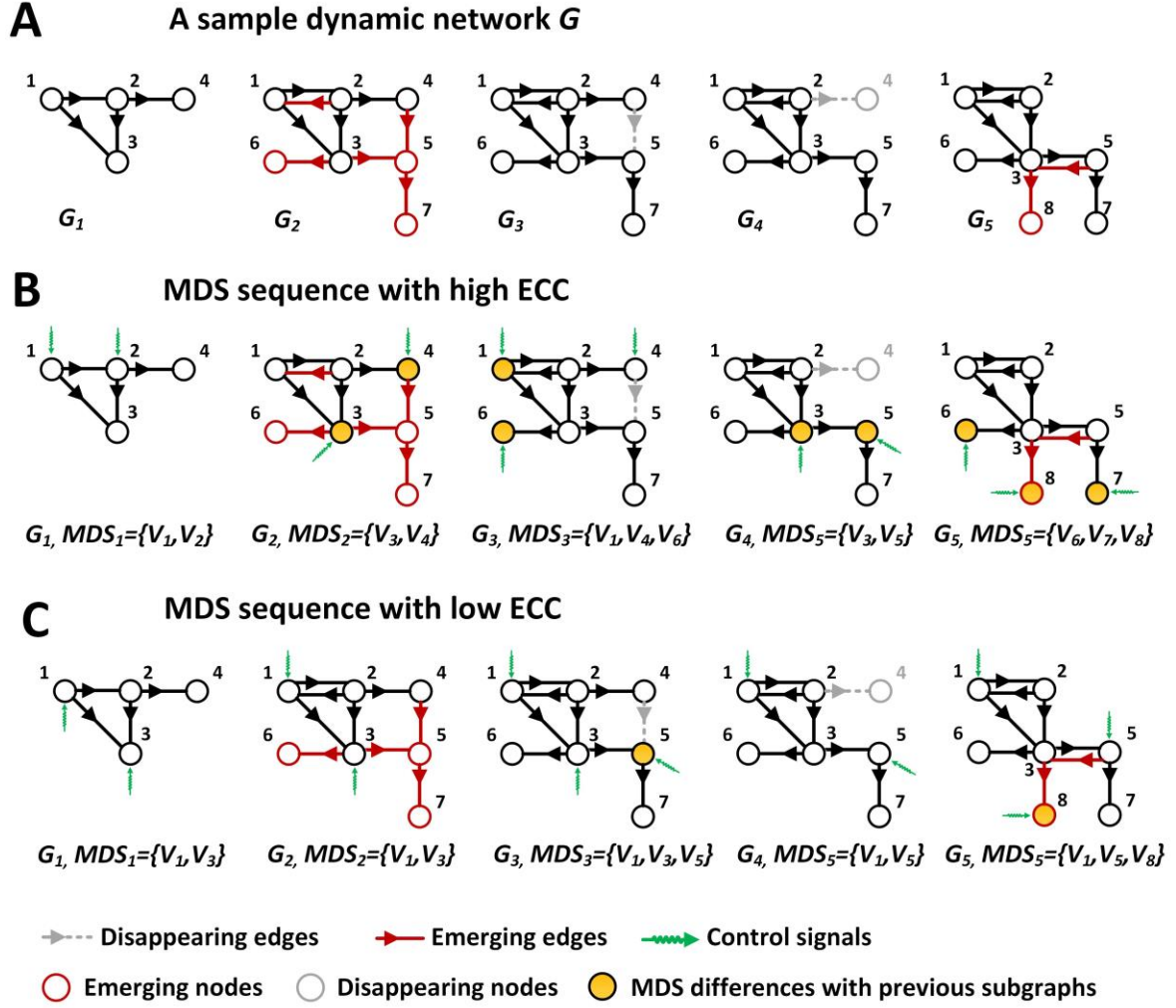


Figure 3. Different MDS sequences of a network. (A) A sample dynamic network with five temporal subgraphs. (B) An MDS sequence with a high ECC, where eight driver nodes are required to control all five temporal subgraphs and nine driver node swappings between neighboring subgraphs are needed; (C) An MDS sequence with a low ECC, where four driver nodes and two driver node swappings are sufficient to control the five temporal subgraphs.

B. Adaptive control metric of nodes

We introduce an adaptive control metric to materialize these two principles in an MDS algorithm to minimize the variations to the resulting MDS and reduce the objective ECC. The adaptive control metric is designed to measure the stability and consistency of nodes in the current MDS with respect to historical network topologies. Following the stability principle, we measure the stability of node v by two factors: 1) the number of edges that node v has in the current and all previous temporal subgraphs, i.e., the degree of node v ; 2) the similarity of edges that node v has in adjacent temporal subgraphs. Specifically, the larger a node degree is, the more neighboring nodes the node interacts with, suggesting the node is more stable [38, 39]. On the other hand, regardless of node degree, a node is also stable if its edges never change [40]. Therefore, we compute the similarity of edges that node v has in neighboring temporal subgraphs as $S_t(v) = \frac{|E_t(v) \cap E_{t-1}(v)|}{|E_t(v) \cup E_{t-1}(v)|}$, where $E_t(v)$ denotes the edge set of node v in temporal subgraph G_t . To sum up, the stability $\sigma_t(v)$ of node v in the current temporal subgraph G_t can be computed as follows:

$$\sigma_t(v) = S_t(v) * DC_t(v), \quad t > 1$$

where $S_t(v) \in [0,1]$ is the edge similarity of node v in adjacent subgraphs. $DC_t(v) = \frac{\sum_j x_{v,j}(t)}{N(t)-1} \in [0,2]$ is the degree centrality of node v at the time t , where $x_{v,j}(t)$ indicates whether nodes v and j are connected at time t , and $N(t)$ is the number of nodes in G_t . As G_t is directed, the bidirectional edges are counted twice; thus, the range of degree centrality is $[0, 2]$.

Furthermore, as the network evolves continuously, we consider the stability of node v over a period. We take the total stability of node v across l immediately previous temporal subgraphs as the final stability measure. The final stability $stb_t(v)$ of node v in the current temporal subgraph G_t can be computed as:

$$stb_t(v) = \sum_{i=t-l}^t \sigma_i(v) \quad (1)$$

To increase consistency between the MDSs of adjacent subgraphs (by the consistency principle), we prefer to keep the driver nodes in the last subgraph as the driver nodes of the current subgraph if possible. Thus, the node consistency measure q_v of G_t is given as:

$$q_v = 2l * P_{t-1}(v) + stb_t(v) \quad (2)$$

where $P_{t-1}(v)$ indicates whether node v appears in the previous MDS, which is 1 if v appears in the previous MDS or 0 otherwise:

$$P_{t-1}(v) = \begin{cases} 1, & v \in MDS_{t-1} \\ 0, & v \notin MDS_{t-1} \end{cases} \quad (3)$$

We give the consistency principle greater importance than the stability principle, i.e., a node that appeared in the last MDS is prioritized as a driver node over nodes with high stability. The node consistency q_v has the following feature:

Property 1: Given two nodes v_1 and v_2 in a temporal subgraph G_t , if $v_1 \in MDS_{t-1}$ and $v_2 \notin MDS_{t-1}$, then $q_{v_1} > q_{v_2}$.

Proof: Since $S_t(v)$ is bounded between 0 and 1, and $DC_t(v)$ between 0 and 2, the stability $stb_t(v)$ of any node v will range from 0 to $2l$. From equations (2) and (3), q_{v_1} will range from $2l$ to $4l$ because v_1 is in the previous MDS. On the other hand, q_{v_2} will be between 0 and $2l$ since v_2 is not included in the previous MDS. The maximum value of q_{v_2} can only reach $2l$, which is the minimum possible value for q_{v_1} . To demonstrate that the maximum value of q_{v_2} cannot be equal to the minimum value of q_{v_1} , consider the following scenario: if $q_{v_1} = q_{v_2} = 2l$, then $stb_t(v_1) = 0$, implying that the stability of v_1 is zero over the previous l subgraphs. This scenario may only occur if either the degree centrality $DC_t(v_1)$ or the edge similarity $S_t(v_1)$ is zero in every preceding l subgraph. Meanwhile, $stb_t(v_2) = 2l$ means that v_2 has a degree centrality of 2 consistently across the previous l subgraphs. However, for v_2 to have a degree centrality of 2, it must maintain constant connections, including connecting to v_1 . This is contradictory with the situation where the degree centrality or edge similarity must be zero, as they would not connect to v_2 . Thus, the two conditions are mutually exclusive, confirming that q_{v_1} must always be greater than q_{v_2} , proving the property.

C. Adaptive control algorithm

We develop the Adaptive Control (AC) algorithm to minimize the total cost of controlling a dynamic network. The algorithm is tailored to ensure consistency between the MDSs of sequential temporal subgraphs, namely the preceding subgraph G' and the current subgraph G . A pivotal aspect of our approach is the integration of the adaptive control metric for nodes. This metric is used to prioritize nodes in computing maximum matching, ensuring an efficient and systematic approach to managing network dynamics.

In a nutshell, the AC algorithm leverages the incumbent maximum matching M' from the previous graph G' to efficiently derive the maximum matching M for the updated graph G . This algorithmic strategy is particularly beneficial when the graph undergoes minor and incremental changes, thereby minimizing disruption to its overall controlling structure. The algorithm focuses on the difference between G' and G by finding edges in M' that are missing in G and vice versa. Starting from the existing partial matching M' , it then systematically searches for augmenting paths to convert G' to G using the differential edges between G' and G . This procedure is iteratively executed until the maximum matching for G is determined.

Throughout this maximum matching process, the adaptive control metric is instrumental in ordering the nodes to be explored. This metric provides a well-defined strategy for node prioritization. The Breadth-First Search (BFS) algorithm, adopted in this phase, employs this node ordering to explore paths that engage more stable nodes. This focused approach not only addresses specific node preferences but also diligently maintains the coherence and consistency of the matching framework, adapting to the dynamic nature of the graph. The pseudocode of the algorithm is listed in ALGORITHM 1.

Figure 4 illustrates the AC algorithm on an example dynamic network. Initially, in temporal subgraph G_1 , the metric $\{q_1 = 0, q_2 = 0, q_3 = 0, q_4 = 0\}$ is calculated by formula (2), resulting in an MDS of $\{v_3, v_4\}$. Subsequently, when the network evolves to G_2 , the node metric q is recalculated by formula (2), and an augmenting path search is performed by prioritizing the metric q in descending order, leading to an MDS of $\{v_3, v_4\}$ (Figure 4A). This procedure is repeated until the network no longer undergoes any further changes.

We illustrate the new maximum matching using the temporal subgraph G_2 (Figure 4B). Initially, the matching edges in the previous temporal subgraph G_1 will be set as the initial matching edges of G_2 in the bipartite graph b_0 (i.e., edge $v_1 \rightarrow v_2$ and edge $v_2 \rightarrow v_1$), and the node search order is set to $\{v_7, v_6, v_5, v_1, v_2, v_4, v_3\}$. Next, the augmenting path of v_7 is searched for, resulting in b_1 . This is followed by searching for the augmenting path of v_6 , reaching b_2 . Subsequently, searching for an augmenting path of v_5 ends in b_3 . Note that although v_1 and v_2 have already been matched at the beginning, once there is an augmented path connected to them in the process of b_1 - b_3 , v_1 and v_2 will no longer be matched. As a result, the unmatched nodes $\{v_3, v_4\}$ are determined to be the MDS of the temporal subgraph G_2 .

IV. EXPERIMENTAL RESULTS AND ANALYSIS

A. Network datasets

We comprehensively evaluated the AC algorithm on synthetic and real-world networks. A total of 1,860 synthetic networks were constructed based on two well-known models: the Scale-Free (SF) model [41] and the Erdős-Rényi (ER) model [42]. We first utilized the SF model to generate 31 static network instances. Each of the instances contains 10,000 nodes. The average degree of the networks varied from 2.0 to 8.0 with an increment of 0.2 while holding the degree exponent constant at 3. Subsequently, 100 temporal subgraphs were created for each of these 31 static instances by partially reconnecting edges randomly with the degree exponent set to 3. The reconnection was determined by 30 reconnection ratios r , which varied between 0.01 and 0.30 in steps of 0.01. As a result, a total of $31 \times 30 = 930$ dynamic network instances were generated for the SF model, each consisting of 100 temporal subgraphs. Similarly, for the ER model, we followed the identical procedure as described for the SF model, except reconnection was completely random, resulting in an additional 930 network instances. In summary, our experiments encompassed a vast synthetic dataset originating from the SF and ER models, providing a robust foundation for evaluating the efficacy of our algorithm.

We also analyzed AC on 20 real-world dynamic networks, including *email*, *human contact*, and *social* networks, which were sourced from previous studies (Table 1) [43-45]. These networks possess a variety of topologies, temporal patterns, and interaction complexities, making them particularly suitable for evaluating dynamic network control algorithms. Their diverse characteristics, spanning from smaller, focused group interactions to larger, complex structures, accommodate thorough benchmarking across different scales and scenarios. These testbeds not only validate our new algorithm but showcase it in many real-world applications.

ALGORITHM 1: Adaptive Control Algorithm

1. **Input:** current temporal subgraph G ; previous temporal subgraph G' ; previous matching M' ; previous MDS $preMDS$; parameter l ;
 2. **Output:** current MDS MDS ; current matching M ;
// Step1 RemoveEdgeFromMatching
 3. removed_edges = getRemovedEdges(G, G')
// Remove edges from M' that are no longer in G
 4. **For** edge in removed_edges:
 5. **If** edge in M' :
 6. removeFromMatching(M' , edge)
 7. // Step2 CalculateAdaptiveControlMetric
 7. **For** each node v in G :
 8. stability = degreeCentrality[v] * edgeSimilarity[v]
 9. $P[v] = 1$ if v in $preMDS$ else 0
 10. $q[v] = 2 * l * P[v] + stability$
 11. // Step3 GetNewMDS
 11. $MDS, M = \text{GetMDS}(G, M', q)$
 12. **Function** GetMDS(G, M', q)
 13. **Get** order q' by ascending weight vector q ;
 14. **Repeat**
 15. **Get** unmatched nodes set un by matching M' ;
 16. **For** node n in un by order q' :
 17. **If** node n has the augmenting paths then:
 18. Expand the augmenting paths and obtain a new matching M^* ;
 19. **Find** all unmatched nodes un' after matching;
 20. **Let** $M = M^*$;
 21. **Let** $MDS = un'$;
 22. **Until** no augmenting path is found;
 23. **Return** $MDS; M$;
-

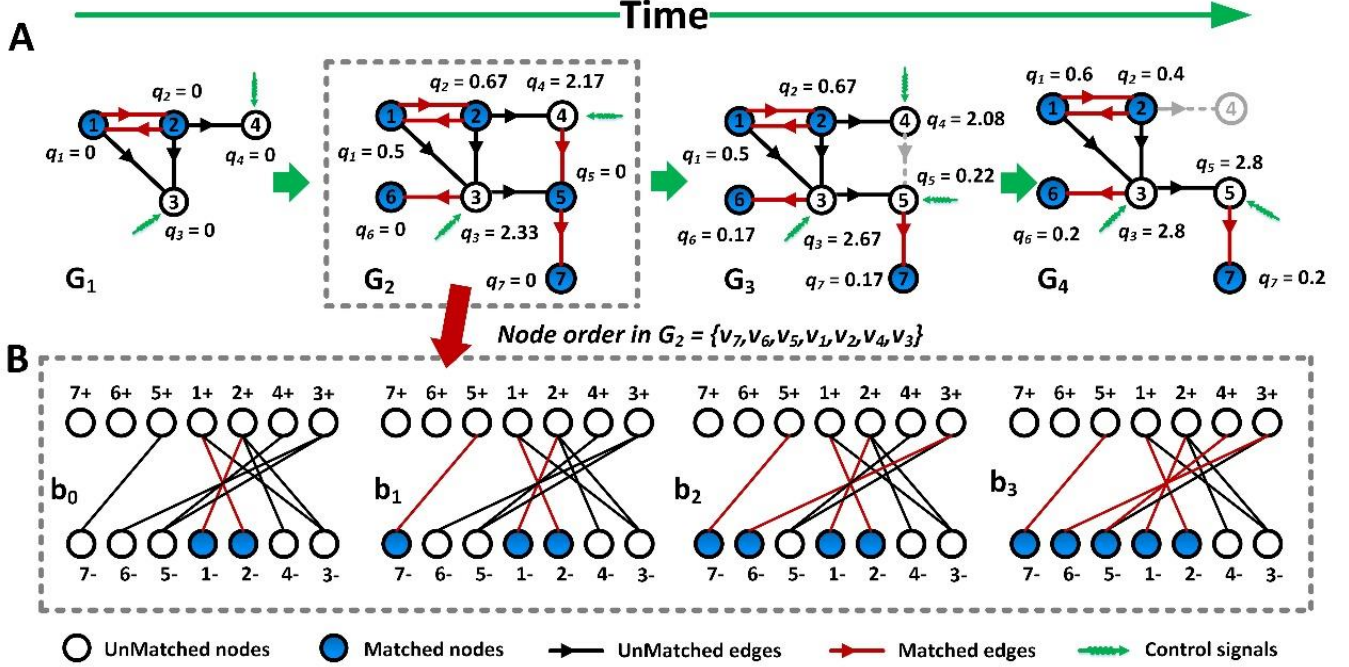


Figure 4. An AC algorithm instance. (A) A simple dynamic network with four temporal subgraphs. (B) The process of maximum matching repair method on G_2 . In this instance, the parameter l of the adaptive control metric is 1.

Table 1. Real dynamic networks dataset. N_{mean} is the mean number of nodes in the real dynamic network; N_{min} and N_{max} are the minimum and maximum numbers of nodes in the network, respectively. K_{mean} is the mean value of the average degree of all temporal subgraphs of the dynamic network. K_{min} and K_{max} are the minimum and maximum average degrees of the network, respectively. T is the number of temporal subgraphs contained in the dynamic network.

Type	Dynamic Networks	N_{mean}	N_{min}	N_{max}	K_{mean}	K_{min}	K_{max}	T
Email	<i>email-Eu-core-temporal</i>	763.22	738	818	19.62	17.79	21.93	9
	<i>email-Eu-core-temporal-Dept1</i>	231.67	219	239	9.94	8.81	11.99	9
	<i>email-Eu-core-temporal-Dept2</i>	120.78	115	127	13.28	11.57	14.55	9
	<i>email-Eu-core-temporal-Dept3</i>	72.67	66	81	11.94	10.32	13.56	9
	<i>email-Eu-core-temporal-Dept4</i>	108.11	102	120	11.36	9.44	12.63	9
	<i>ia-radoslaw-email</i>	93.94	2	140	7.64	1.0	14.89	118
	<i>sx-mathoverflow</i>	2038.02	812	2461	7.93	3.46	14.77	40
	<i>sx-mathoverflow-a2q</i>	1532.75	403	1866	3.36	1.48	8.49	40
	<i>sx-mathoverflow-c2a</i>	1185.18	356	1433	4.71	2.10	9.26	40
	<i>sx-mathoverflow-c2q</i>	1285.4	384	1628	5.01	2.90	7.45	40
Social	<i>sx-superuser</i>	5642.14	39	10246	4.07	1.6	10.24	93
	<i>sx-superuser-a2q</i>	4032.52	19	6429	2.33	1.26	6.23	93
	<i>sx-superuser-c2q</i>	2171.78	2	4352	3.04	1.0	3.71	93
	<i>fb-forum</i>	434.5	109	728	4.86	2.11	12.59	10
	<i>CollegeMsg</i>	631.86	200	1371	7.35	2.37	15.012	7
Human contact	<i>contacts-prox-high-school-2013</i>	291.33	232	312	12.90	5.68	16.6	6
	<i>edit-enwikibooks</i>	3453.56	2	14451	1.97	1.0	2.48	139
	<i>copresence-LH10</i>	31.54	10	48	15.32	3.4	26.65	13
	<i>ia-workplace-contacts</i>	73.75	62	87	6.82	3.03	10.94	4
	<i>ia-hospital-ward-proximity-attr</i>	42	32	49	12.56	6.94	17.49	8

B. Performance metric and benchmark algorithm for comparison

The temporal subgraphs of a real network may follow variable rates of change. These fluctuations may significantly affect algorithm performance. To probe into this issue, we adopted the Jaccard index as a measure to assess the overlap between nodes in consecutive temporal subgraphs of an evolving network to evaluate the consistency of edges. In particular, we employed the Jaccard similarity coefficient [46] to quantify the node similarity and structural similarity between neighboring temporal subgraphs, expressed as

$$J(A, B) = \frac{|A \cap B|}{|A \cup B|}$$

where A and B are the node sets (or edge sets) of subgraphs G_{i-1} and G_i , respectively.

To establish a sound benchmark to evaluate our adaptive control strategy and algorithm, we revised and enhanced an algorithm originally designed for static networks proposed by *Liu et al.* [14]. Specifically, we adopted the maximum matching-based (MM), which has been demonstrated to be state-of-the-art in computing the MDS for static networks. The MM algorithm will be applied to each temporal subgraph of the dynamic network, and eventually, the same MDS sequence as the AC algorithm can be obtained. Using the MM algorithm as the comparison benchmark has several advantages. Firstly, adaptive control is a completely new problem, and there is still no suitable algorithm to solve it. Secondly, MM computes exact solutions for the MDS problem, which is critically important for dynamic network control. In contrast, many existing dynamic network control algorithms compute approximate MDS solutions, often resulting in suboptimal control performance [27-30]. Furthermore, the revised MM algorithm does not rely on knowledge of network changes over time. This characteristic aligns well with the scenario we consider where knowledge of network alterations is typically unavailable. In contrast, many dynamic control algorithms require a comprehensive understanding of the entire network's temporal dynamics, which can be a significant limitation in practice [27-30].

C. Results on synthetic networks

The AC and MM algorithms were first experimentally compared on synthetic dynamic networks (Figure 5). The Extra Control Costs (ECCs) for the AC algorithm, ECC_{AC} , the MM algorithm, ECC_{MM} , and their ratio ECC_{AC}/ECC_{MM} were computed. AC consistently outperformed MM on synthetic ER and SF networks with varying reconnection ratio r and average degree k , achieving $ECC_{AC}/ECC_{MM} < 1$ on the two types of synthetic networks we tested (Figure 5). A smaller ECC_{AC}/ECC_{MM} ratio indicates that AC outperforms MM. Notably, on stable networks (with reconnection ratio $r < 0.1$), the AC was nearly twice as effective as the MM algorithm, spending almost half of the ECC. Even with an increasing reconnection ratio r , the AC algorithm outperformed MM across networks with varied average degrees. Furthermore, similar optimization outcomes across various parameter l values indicated a specific trend in MDS optimization selection. It appeared that the MDS optimization selection might depend on network topological structures and that of the immediately preceding temporal subgraph. Consequently, there is no need to retain the full history of topology, which enhanced the efficiency of the algorithm and broadened its applicability.

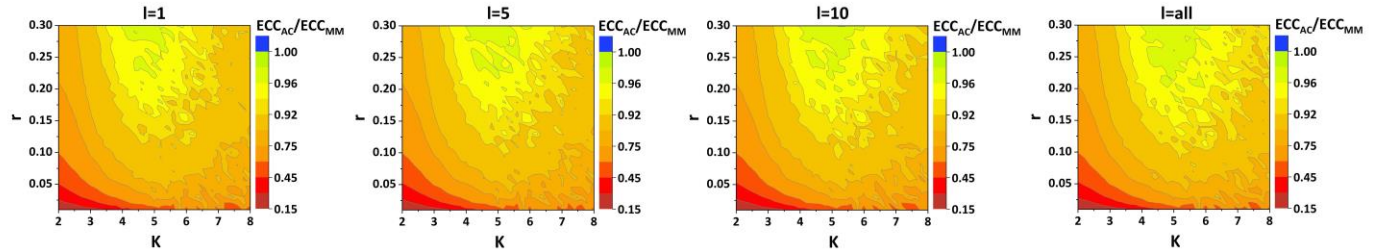
Moreover, the AC algorithm was more efficient on SF-based dynamic networks, averaging a ratio of $ECC_{AC}/ECC_{MM} = 0.72$, than on ER-based dynamic networks, with an average $ECC_{AC}/ECC_{MM} = 0.84$. This variance can be primarily attributed to the unique characteristics inherent to each network model. As per Equation (2), the AC algorithm preferentially favors nodes with greater stability. It aligns well with the power-law distribution trait in the SF model. In contrast, the ER model's random evolution cannot satisfy this characteristic, particularly when the reconnection ratio r is large. Moreover, while AC's performance deteriorates with increasing reconnection ratio r , the decrement is more subtle for SF-based networks than ER-based networks.

We conducted an in-depth analysis at the temporal subgraph level to investigate the efficacy of our algorithm further. We compared the ECCs of the AC and MM algorithms on temporal subgraphs (Figure 6). The results on the ER-based dynamic networks showed that AC outperformed MM for 95% of the temporal subgraphs when the average degree k was less than 4 (Figure 6A). However, as the average degree k surpassed 4, temporal subgraphs displaying equivalent performance between the two algorithms increased (yellow part in Figure 6A). The results on the SF-based dynamic networks were compatible with those on the ER networks. The AC algorithm was superior to MM in 100% of the temporal subgraphs with an average degree k below 6. As the average degree increases, the two algorithms performed similarly on more temporal subgraphs (yellow part in Figure 6B).

Interestingly, as network density increased, the discernible advantage of the AC algorithm relative to MM diminished. This is not indicative of AC's inadequacy for dense networks. When networks became denser, the MDS sizes decreased significantly (supplementary material). This reduction led to a constrained optimization space for the MDS within each temporal subgraph. As a result, both MM and AC algorithms may produce similar solutions. For instance, the mean ECC_{AC}/ECC_{MM} ratio of ER-based dynamic networks was 0.63 when $k=2.0$ and elevated to 0.85 when $k=8.0$ (supplementary material). We showed two extreme cases of temporal subgraphs where the efficiency of the AC algorithm was the same as or lower than that of the MM algorithm (supplementary material). They respectively explained the situations when the two algorithms performed equally and when MM outperformed AC. In fact, on ER-based networks, the two algorithms performed almost the same once the network reconnection ratio exceeded 0.50.

In dynamic networks with a high change rate in neighboring temporal subgraphs, the AC algorithm's performance does not continuously worsen with an increased change rate. Instead, it has a lower-bound performance equivalent to the MM algorithm. Because the latter searches for augmenting paths in a fixed or random order, which is unbiased. When the adaptive control metric in AC becomes ineffective due to the high change rate, AC will behave the same as MM and perform matching by the default order. In this case, even if there is a slight discrepancy in the ECC results of the two algorithms in a single temporal subgraph, the overall ECC of the dynamic network will be similar.

A Result of ER-based dynamic network



B Result of SF-based dynamic network

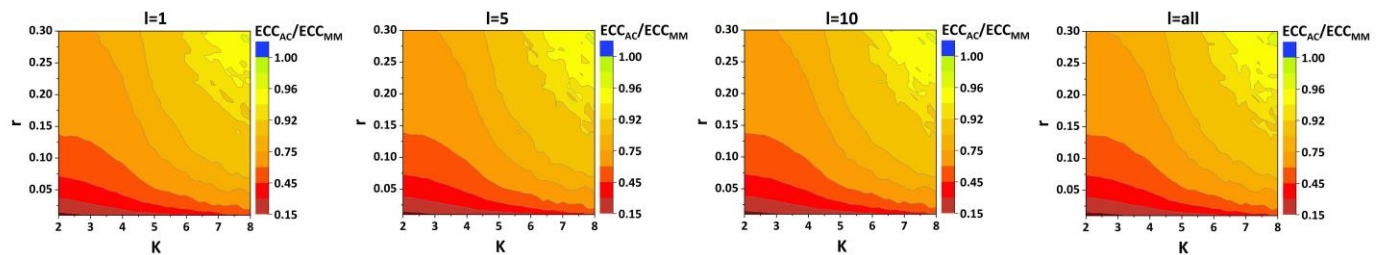


Figure 5. The ECC results of the AC and MM algorithms on synthetic networks. (A) The result on ER-based dynamic networks. (B) The result on SF-based dynamic networks. The horizontal axis represents the average degree k of the network, and the vertical axis represents the reconnection ratio r . The color scale indicates the value of the ratio ECC_{AC}/ECC_{MM} , with smaller values indicating superior algorithmic performance.

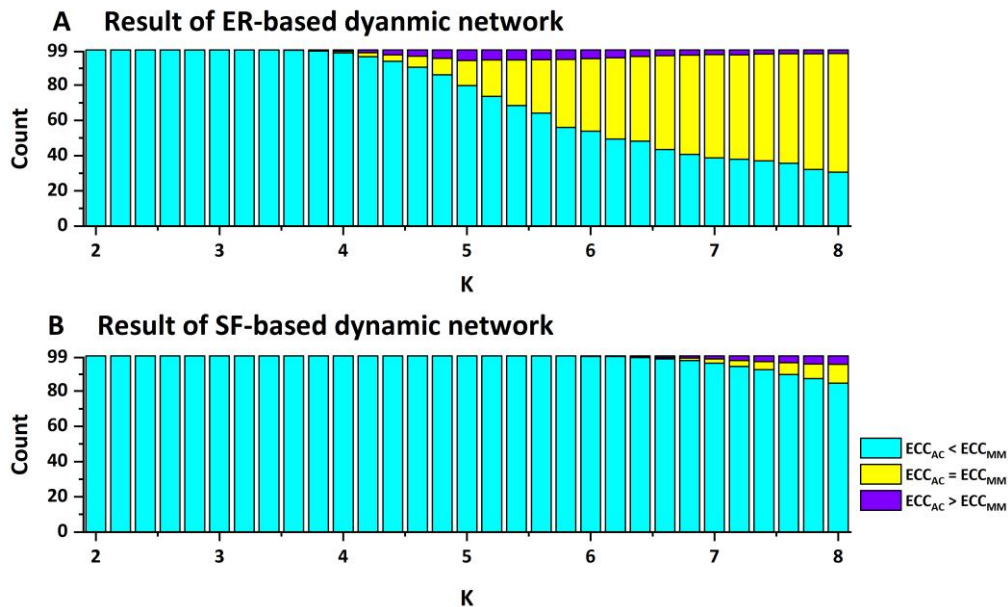


Figure 6. Performance of the AC algorithm on all temporal subgraphs. (A) The performance of the AC on all temporal subgraphs in an ER-based dynamic network. (B) The performance of the AC on all temporal subgraphs in an SF-based dynamic network. The horizontal axis represents the average degree k of the network. The vertical axis represents the average number of temporal subgraphs. For any given average degree k , the average temporal subgraphs are computed based on the average count of all temporal subgraphs with different reconnection ratios r and different numbers of pre-sequence temporal subgraphs considered l .

D. Results on real networks

We evaluated the AC and other algorithms on a diverse set of 20 real dynamic networks, chosen based on their topological structures and dynamic changes. The use of these networks was to ensure that the algorithms were evaluated across a wide range of conditions to gain a deep understanding of their generality and efficacy on real-world networks.

We computed the ECCs for the AC and MM algorithms on the 20 real networks. The results showed that AC outperformed MM, boasting the ECC_{AC}/ECC_{MM} ratio by 0.81 on average across all networks (Table 2). However, the performance of AC varied significantly across different networks. For example, on the *email-Eu-core-temporal* and *contacts-prox-high-school-2013* networks, AC performed significantly better than MM, resulting in $ECC_{AC}/ECC_{MM}=0.50$. Conversely, AC and MM have similar performance on highly dynamically changing networks, like *sx-superuser* and *edit-enwikibooks* (Table 2).

To further understand the varying performance of the AC algorithm on different networks, we studied the dynamic network characteristics. We calculated the node and edge similarities of consecutive subgraphs as a representation of the network's dynamism (see Section *Performance metric and benchmark algorithm for comparison*). On networks exhibiting low dynamism, characterized by higher node and edge similarities, AC significantly outperformed MM. However, as the dynamism of the networks increased, the efficacy of AC declined. There is a negative correlation between the ECC_{AC}/ECC_{MM} ratio and node and edge similarities (Figure 7). The higher the average similarity in consecutive subgraphs, the better that AC would perform. This phenomenon can be attributed to the fact that when there are drastic alterations in neighboring subgraphs, the fundamental objective of the AC optimization algorithm—aiming to maintain the same driver nodes as the original MDS—becomes challenging to achieve, resulting in a performance dip. However, in scenarios where the network undergoes gradual changes, AC distinctly surpasses MM, attesting to the efficacy of the AC algorithm.

Using the same analytic strategy as used for synthetic networks, we also analyzed the temporal subgraphs to understand AC's performance on real-world networks. Notably, AC exhibited superior performance over MM across all temporal subgraphs in 11 out of the 20 real networks analyzed (Figure 8). For 17 of these 20 networks, AC surpassed MM in over 80% of the temporal subgraphs. Figure 9 shows a more detailed view of the results for each temporal subgraph. Note that AC's performance fluctuates across different temporal subgraphs, even within the same real dynamic network (Figure 9).

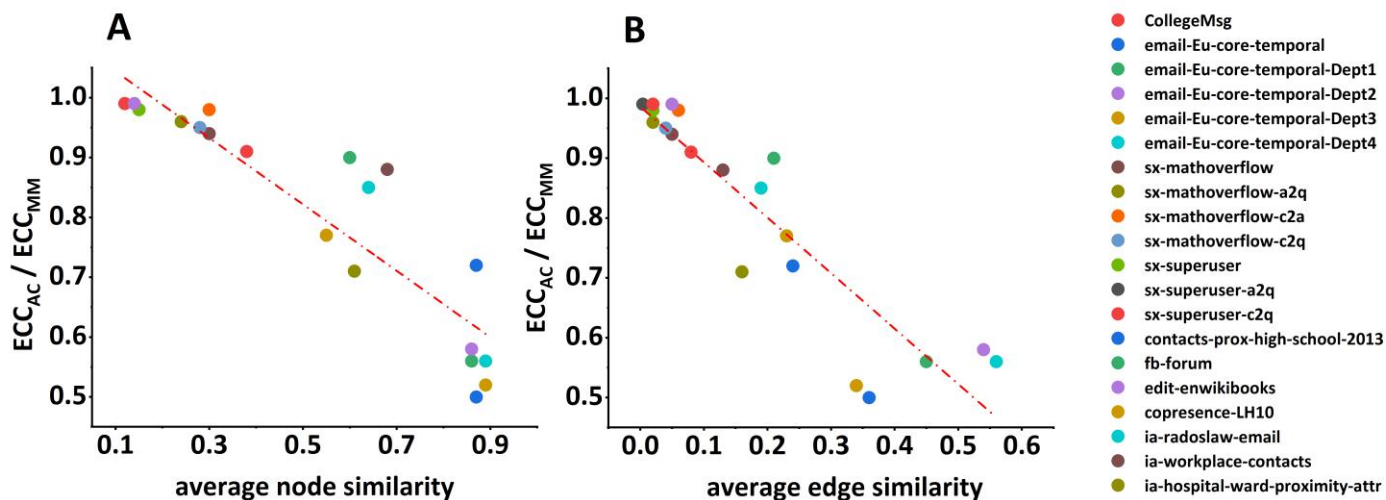


Figure 7. Relationship between AC algorithm performance and similarity of temporal subgraphs in real networks. (A) The relationship between the average node similarity and AC algorithm performance. (B) The relationship between the average edge similarity and AC algorithm performance. The smaller ECC_{AC}/ECC_{MM} means the higher algorithm performance.

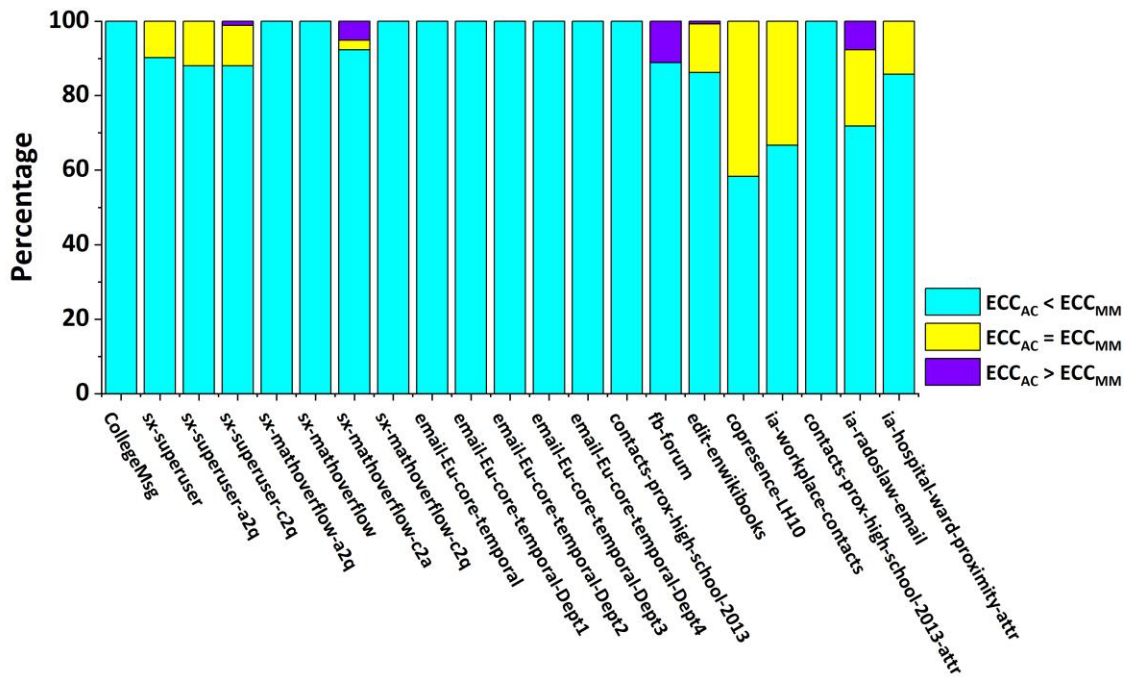


Figure 8. Performance of the AC algorithm on temporal subgraphs in real networks. The vertical axis represents the temporal subgraph ratio in different real networks.

Table 2. Results on real networks. S_n and S_e denote the mean similarities of the node and edge of the networks, respectively.

Dynamic Networks	S_n	S_e	Average MDS	ECC_{AC}	ECC_{MM}	ECC_{AC}/ECC_{MM}
CollegeMsg	0.38	0.08	236.71	934	1023	0.91
email-Eu-core-temporal	0.87	0.36	148.33	406	811	0.5
email-Eu-core-temporal-Dept1	0.86	0.45	55.78	154	275	0.56
email-Eu-core-temporal-Dept2	0.86	0.54	20.11	68	117	0.58
email-Eu-core-temporal-Dept3	0.89	0.34	13.78	43	82	0.52
email-Eu-core-temporal-Dept4	0.89	0.56	16.44	55	99	0.56
sx-mathoverflow	0.3	0.05	694	21508	22919	0.94
sx-mathoverflow-a2q	0.24	0.02	874.1	24279	25320	0.96
sx-mathoverflow-c2a	0.3	0.06	578.9	18246	18536	0.98
sx-mathoverflow-c2q	0.28	0.04	498	12018	12634	0.95
sx-superuser	0.15	0.02	2496.41	207738	211540	0.98
sx-superuser-a2q	0.12	0.004	2385.38	189038	191514	0.99
sx-superuser-c2q	0.12	0.02	927.6	67131	68091	0.99
contacts-prox-high-school-2013	0.87	0.24	52.5	96	134	0.72
fb-forum	0.6	0.21	212.6	815	908	0.9
edit-enwikibooks	0.14	0.05	2962.58	334285	337951	0.99
copresence-LH10	0.55	0.23	4.85	33	43	0.77
ia-radoslaw-email	0.64	0.19	22.22	1706	2017	0.85
ia-workplace-contacts	0.68	0.13	20	37	42	0.88
ia-hospital-ward-proximity-attr	0.61	0.16	15.5	45	63	0.71

V. CONCLUSION

In this study, we proposed a dynamic control method, *adaptive control* (AC), for finding effective control schemes for dynamic networks in real time. The novel AC algorithm was evaluated on synthetic and real networks. A major result of our study is that the similarity of the consecutive temporal subgraphs that represent the evolving dynamics of a dynamic network has a great impact on how the network should be controlled and the performance of the AC algorithm. We also analyzed the performance bound of the AC algorithm, showing that AC outperformed the baseline maximum matching-based (MM) algorithm on most dynamic networks that we analyzed. This study has not only provided an effective and practical method for adaptively controlling dynamic networks but also deepened our understanding of dynamic network control and opened new venues for network research and applications.

AUTHOR CONTRIBUTION

XZ conceived the study and drafted manuscript. WZ revised the manuscript. CP, CZ and HZ implemented the algorithm, performed data analysis, prepared the figures and drafted the manuscript. ZS collated the data and revised the figures. All authors contributed to the preparation of the manuscript.

ACKNOWLEDGMENT

This work was supported by the National Natural Science Foundation of China [grant number 62176129], the National Key Research and Development Program of the Ministry of Science and Technology of China [grant number 2022YFC2405603], and the Strategic Topic Grant scheme of Hong Kong [grant number STG1/M-501/23-N].

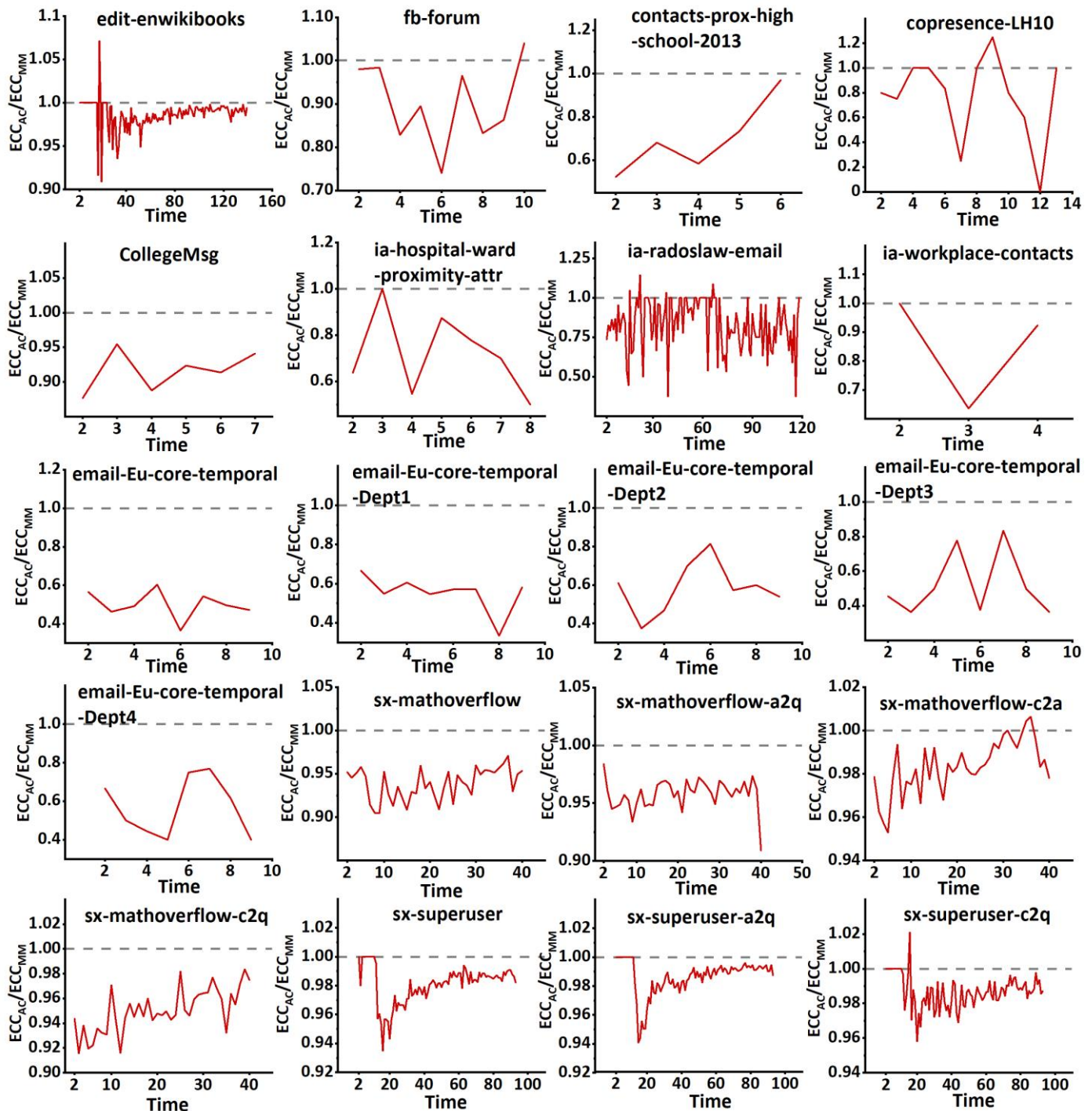


Figure 9. Optimization of the ECC for temporal subgraphs in real networks. The horizontal axis represents the temporal subgraphs at different time points, and the vertical axis represents the ECC ratios between the AC and MM algorithms. The gray

dashed line with $y=1$ serves as the baseline, where the region above the line, i.e., $ECC_{AC}/ECC_{MM} > 1$, indicates the occurrence of negative optimization.

REFERENCES

- [1] M. E. J. Newman, "The structure and function of complex networks," *SIAM review*, vol. 45, no. 2, pp. 167-256, 2003.
- [2] S. Boccaletti, V. Latora, Y. Moreno, M. Chavez, and D. U. Hwang, "Complex networks: Structure and dynamics," *Physics reports*, vol. 424, no. 4-5, pp. 175-308, 2006.
- [3] S. H. Strogatz, "Exploring complex networks," *nature*, vol. 410, no. 6825, pp. 268-276, 2001.
- [4] C. Pan et al., "Control Analysis of Protein-Protein Interaction Network Reveals Potential Regulatory Targets for MYCN," *Front Oncol*, vol. 11, p. 633579, 2021, doi: 10.3389/fonc.2021.633579.
- [5] Z. Xizhe, "Altering indispensable proteins in controlling directed human protein interaction network," *IEEE/ACM Transactions on Computational Biology Bioinformatics*, pp. 1-1, 2018.
- [6] X. Zhang et al., "Cancer-keeper genes as therapeutic targets," *iScience*, 2023.
- [7] X. Wei, C. Pan, X. Zhang, and W. Zhang, "Total network controllability analysis discovers explainable drugs for Covid-19 treatment," *Biology Direct*, vol. 18, no. 1, p. 55, 2023.
- [8] C. S. Kim, "Free energy and inference in living systems," *Interface Focus*, vol. 13, no. 3, p. 20220041, 2023.
- [9] D. Zhou et al., "Mindful attention promotes control of brain network dynamics for self-regulation and discontinues the past from the present," *Proceedings of the National Academy of Sciences*, vol. 120, no. 2, p. e2201074119, 2023.
- [10] X. He et al., "Uncovering the biological basis of control energy: structural and metabolic correlates of energy inefficiency in temporal lobe epilepsy," *Science Advances*, vol. 8, no. 45, p. eabn2293, 2022.
- [11] M. Bardoscia et al., "The physics of financial networks," *Nature Reviews Physics*, vol. 3, no. 7, pp. 490-507, 2021.
- [12] L. F. Seoane, "Games in rigged economies," *Physical Review X*, vol. 11, no. 3, p. 031058, 2021.
- [13] A. Ciullo, E. Strobl, S. Meiler, O. Martius, and D. N. Bresch, "Increasing countries' financial resilience through global catastrophe risk pooling," *Nature Communications*, vol. 14, no. 1, p. 922, 2023/02/17 2023, doi: 10.1038/s41467-023-36539-4.
- [14] Y. Y. Liu, J. J. Slotine, and A. L. Barabasi, "Controllability of complex networks," *Nature*, vol. 473, no. 7346, pp. 167-73, May 12 2011, doi: 10.1038/nature10011.
- [15] R. M. D'Souza, M. di Bernardo, and Y.-Y. Liu, "Controlling complex networks with complex nodes," *Nature Reviews Physics*, vol. 5, no. 4, pp. 250-262, 2023.
- [16] G. Baggio, D. S. Bassett, and F. Pasqualetti, "Data-driven control of complex networks," *Nature communications*, vol. 12, no. 1, p. 1429, 2021.
- [17] Y.-Y. Liu and A.-L. Barabási, "Control principles of complex systems," *Reviews of Modern Physics*, vol. 88, no. 3, Sep 6 2016, Art no. 035006, doi: 10.1103/RevModPhys.88.035006.
- [18] X. Zhang, J. Han, and W. Zhang, "An efficient algorithm for finding all possible input nodes for controlling complex networks," *Scientific Reports*, no. 1, 2017.
- [19] J. Ruths and D. Ruths, "Control Profiles of Complex Networks," *Science*, vol. 343, no. 6177, pp. 1373-6, 2014.
- [20] C. Campbell, J. Ruths, D. Ruths, K. Shea, and R. Albert, "Topological constraints on network control profiles," *Sci Rep*, vol. 5, no. 1, p. 18693, Dec 22 2015, doi: 10.1038/srep18693.
- [21] X. Zhang, H. Wang, and T. Lv, "Efficient target control of complex networks based on preferential matching," *PLoS One*, vol. 12, no. 4, p. e0175375, 2017, doi: 10.1371/journal.pone.0175375.
- [22] X. Zhang, T. Lv, X. Yang, and B. Zhang, "Structural controllability of complex networks based on preferential matching," *PLoS One*, vol. 9, no. 11, p. e112039, Nov 6 2014, Art no. e112039, doi: 10.1371/journal.pone.0112039.
- [23] X. Zhang, Y. Zhu, and Y. Zhao, "Altering control modes of complex networks by reversing edges," *Physica A: Statistical Mechanics and its Applications*, vol. 561, no. C, p. 125249, 2021.
- [24] X. Zhang and Q. Li, "Altering control modes of complex networks based on edge removal," *Physica A: Statistical Mechanics and its Applications*, vol. 516, 2019.
- [25] A. Li, S. P. Cornelius, Y. Y. Liu, L. Wang, and A. L. Barabasi, "The fundamental advantages of temporal networks," *Science*, vol. 358, no. 6366, pp. 1042-1046, Nov 24 2017, doi: 10.1126/science.aai7488.
- [26] Y. Cui, S. He, M. Wu, C. Zhou, and J. Chen, "Improving the Controllability of Complex Networks by Temporal Segmentation," *IEEE Transactions on Network Science Engineering*, vol. PP, no. 99, pp. 1-1, 2020.
- [27] M. Pósfai and P. Hövel, "Structural controllability of temporal networks," *New Journal of Physics*, vol. 16, no. 12, Dec 22 2014, Art no. 123055, doi: 10.1088/1367-2630/16/12/123055.
- [28] F. M. Babak Ravandi, John A Springer "Identifying and using driver nodes in temporal networks," *Journal of Complex Networks*, vol. Volume 8, Issue 2, April 2020, cnz025, 2019, doi: <https://doi.org/10.1093/comnet/cnz004>.
- [29] Y. Pan and X. Li, "Structural controllability and controlling centrality of temporal networks," *PLoS One*, vol. 9, no. 4, p. e94998, Apr 18 2014, Art no. e94998, doi: 10.1371/journal.pone.0094998.
- [30] P. Yao, B. Y. Hou, Y. J. Pan, and X. Li, "Structural Controllability of Temporal Networks with a Single Switching Controller," *PLoS One*, vol. 12, no. 1, p. e0170584, Jan 20 2017, Art no. e0170584, doi: 10.1371/journal.pone.0170584.
- [31] L. E. C. Rocha, N. Masuda, and P. Holme, "Sampling of temporal networks: Methods and biases," *Phys Rev E*, vol. 96, no. 5-1, p. 052302, Nov 2017, doi: 10.1103/PhysRevE.96.052302.
- [32] E. Almaas, B. Kovacs, T. Vicsek, Z. N. Oltvai, and A. L. Barabasi, "Global organization of metabolic fluxes in the bacterium *Escherichia coli*," (in eng), *Nature*, vol. 427, no. 6977, pp. 839-43, Feb 26 2004, doi: 10.1038/nature02289.
- [33] P. Holme and J. Saramäki, "Temporal networks," *Physics Reports*, vol. 519, no. 3, pp. 97-125, 2012/10/01/ 2012, doi: 10.1016/j.physrep.2012.03.001.
- [34] Kalman and E. R., "Mathematical Description of Linear Dynamical Systems," *Journal of the Society for Industrial*, vol. 1, no. 2, pp. 152-192, 1963.
- [35] J. E. Hopcroft and R. M. Karp, "An $n^5/2$ Algorithm for Maximum Matchings in Bipartite Graphs," vol. 2, no. 4, pp. 225-231, 1973, doi: 10.1137/0202019.
- [36] L. Zdeborová and M. Mézard, "The number of matchings in random graphs," *Journal of Statistical Mechanics: Theory and Experiment*, vol. 2006, no. 05, pp. P05003-P05003, 2006, doi: 10.1088/1742-5468/2006/05/p05003.
- [37] T. Jia and A. L. Barabasi, "Control capacity and a random sampling method in exploring controllability of complex networks," *Sci Rep*, vol. 3, p. 2354, 2013, doi: 10.1038/srep02354.
- [38] A. L. Barabasi and R. E. Crandall, "Linked: The New Science of Networks," *American Journal of Physics*, vol. 71, no. 4, pp. 243-270, 2002.
- [39] R. Albert and A.-L. Barabási, "Statistical mechanics of complex networks," *Reviews of Modern Physics*, vol. 74, no. 1, pp. 47-97, 01/30/ 2002, doi: 10.1103/RevModPhys.74.47.
- [40] V. Martínez, F. Berzal, and J. C. Cubero, "A Survey of Link Prediction in Complex Networks," *Acm Computing Surveys*, vol. 49, no. 4, p. 69, 2016.
- [41] A. L. Barabasi and R. Albert, "Emergence of scaling in random networks," *Science*, vol. 286, no. 5439, pp. 509-12, Oct 15 1999, doi: 10.1126/science.286.5439.509.

- [42] P. Erdős and A. Rényi, "On random graphs I," *Publ. math. debrecen*, vol. 6, no. 290-297, p. 18, 1959.
- [43] P. Panzarasa, T. Opsahl, and K. M. Carley, "Patterns and dynamics of users' behavior and interaction: Network analysis of an online community," *Journal of the American Society for Information Science and Technology*, vol. 60, no. 5, pp. 911-932, May 2009, doi: 10.1002/asi.21015.
- [44] A. Paranjape and A. R. Benson, "Motifs in Temporal Networks (Wsdm'17: Proceedings of the Tenth AcM International Conference on Web Search and Data Mining). 2017, pp. 601-610.
- [45] R. Rossi and N. Ahmed, "The network data repository with interactive graph analytics and visualization," in *Twenty-ninth AAAI conference on artificial intelligence*, 2015.
- [46] P. Jaccard, "Étude comparative de la distribution florale dans une portion des Alpes et des Jura," *Bull Soc Vaudoise Sci Nat*, vol. 37, pp. 547-579, 1901.